Excellent Timing Cherenkov Light Detection for Dual-readout High-granularity Calorimetry

Weiyuan Li[1,*], *James* Freeman[2], *Corrado* Gatto[3], *Daniel* Jeans[4], *Taiki* Kamiyama[1], *Kodai* Matsuoka[4], *Hiroyasu* Ogawa[1], *Wataru* Ootani[1], *Taikan* Suehara[1], and *Tohru* Takeshita[5]

[1]International Center for Elementary Particle Physics, The University of Tokyo, 7-3-1 Hongo, Bunkyo-ku, Tokyo, 113-0033, Japan
[2]Fermi National Accelerator Laboratory, Batavia, Illinois 60510, USA
[3]Northern Illinois University, DeKalb, Illinois, 60115, USA
[4]The High Energy Accelerator Research Organization, 1-1 Oho, Tsukuba, Ibaraki, 305-0801, Japan
[5]Shinshu University, 3-1-1 Asahi, Matsumoto, Nagano, 390-8621, Japan

Abstract. We are developing a Cherenkov detector aiming for applications in the next-generation calorimetry. It is a calorimetry that combines dual-readout and high-granularity with excellent timing capability. This work is to prove the concept of the Cherenkov detector utilizing a resistive plate chamber (RPC) with Diamond-Like Carbon as resistive electrode. The first prototype was tested with β-rays and cosmic-rays. This paper discusses the behavior of the charge spectrum and the time resolution of the first prototype.

1 Introduction

In future accelerator experiments, precise jet energy measurements will be essential. Technological developments are underway to achieve this goal. Among these developments, dual-readout calorimeters [1] and high-granularity calorimeters [2] have been established through a few decades of research. Dual-readout calorimeter improves hadron energy resolution by simultaneously detecting scintillation and Cherenkov light generated by the charged particles in the shower. High-granularity calorimetry separates the shower clusters by each particle in the jet through a highly segmented readout system for the particle flow approach. As a next-generation calorimeter technology, efforts are being made to combine these two calorimeter technologies and incorporate picosecond-timing [3]. This study focuses on the development of a high-granularity, picosecond-timing Cherenkov detector as a sub-detector for the proposed calorimeter.

2 Concept of the Cherenkov detector

The Cherenkov detector is designed to have a highly segmented readout system and excellent time resolution. The design parameters depend on the application of this technology, but we set a readout granularity of approximately 1 cm and a time resolution of approximately 20 ps as the baseline. The challenge lies in achieving this level of detector performance over a large area while maintaining reasonable costs.

2.1 Detector Priciple

The Cherenkov detector is a radiator coupled with a gaseous photomultiplier based on resistive plate chamber (RPC) as shown in Figure 1. When a relativisitic charged particle passes through the radiator, it leaves a cone of Cherenkov photons. On the photocathode, these photons are converted to photoelectrons, which then enter the RPC gap to get amplified. The movement of the charge in the gap induces the current on the readout pad placed on the back of the RPC anode electrode. A highly granular readout can be easily achieved by segmenting the readout pads.

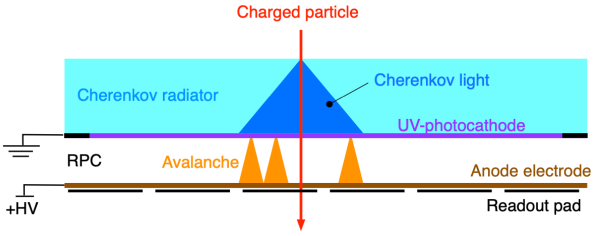

Figure 1. The concept of the Cherenkov detector.

2.2 Radiator

The number of Cherenkov photons N generated by a charged particle per unit length traveled x and per wavelength λ in a radiator is described by

$$\frac{dN}{dxd\lambda} = \frac{2\pi Q^2 \alpha}{\lambda^2} \sin^2 \theta_C,$$

where Q is the charge of the particle, α is the fine-structure constant, and θ_C is the emission angle. To efficiently collect Cherenkov photons, one should select a radiator which is transparent to as short wavelength as possible.

2.3 Gaseous Photomultiplier

The gaseous photomultiplier for this Cherenkov detector is based on RPC which comprises two parallel electrodes with a high electric field applied between them. The cathode electrode is a semi-transparent photocathode so that the photoelectrons reach RPC gap. The wavelength that gives the maximum quantum efficiency should match with the transparent wavelength of radiator.

*e-mail: weiyuan@icepp.s.u-tokyo.ac.jp

The simple structure of RPC based gaseous photomultiplier benefits in low cost and a large area coverage. Additionally, RPCs have a good time resolution on the order of 10 ps with a gap thickness on the order of 100 μm [4].

2.4 DLC-RPC

The drawback of the RPC is its limited rate capability. However, a novel type of high-rate-capable RPC, known as DLC-RPC, has been developed using diamond-like carbon (DLC) as the resistive electrode [5]. It has achieved a rate capability of 1 MHz/cm^2 for low momentum (28 MeV) muons. To make the Cherenkov detector high rate capable, DLC sputtered polyimide foil is used as the anode electrode in this study.

3 Expected Time Resolution

The time variance of Cherenkov photons reaching the photocathode is no more than a few ps, therefore the expected time resolution of the Cherenkov detector is estimated from the measured time resolution of the amplification layer and the number of photoelectrons (#p.e.) generated by MIP.

The time resolution of the amplification layer was evaluated by measuring ionization signal in a stand-alone DLC-RPC. The primary electron of the DLC-RPC signal can be generated anywhere in the gap between the anode and cathode. On the other hand, the primary (photo-)electron of the gaseous multiplier in the Cherenkov detector is generated at the surface of the cathode, and the avalanche develops full range of the gap. As the signal size correlate with the amplification length (if the electric field is the same), we focused on the large size signals of the DLC-RPC. To convert the measured DLC-RPC time resolution to that of the amplification layer, the number of ionization clusters per charged particle, and the number of primary electrons per cluster are considered.

The time resolution of the DLC-RPC with a 192 μm gap thickness was measured using ^{90}Sr β-rays and a time reference counter. The electric field applied in the gaps was 100 kV/cm. A gas mixture of R134a freon with 1% SF_6 and 5% iso-butane was used in the chamber as in Ref. [5]. A time reference counter was placed downstream of the DLC-RPC to trigger events passing through the DLC-RPC. The pulse height slice of the DLC-RPC time resolution is shown in Figure 2. The large signals of DLC-RPC show a time resolution of $\sigma_{\mathrm{RPC}} = 50$–$60$ ps.

A previous study using simulation with a similar gas mixture [6] indicates that a gap thickness of 200 μm is small enough to assume the number of clusters per charged particle is one, and the average number of primary electrons in each cluster is 2.8. If one assumes the signal size scales with the number of primary electrons, the single photoelectron time resolution of the amplification layer, $\sigma_{1\mathrm{pe}}$, is given by

$$\sigma_{1\mathrm{pe}} \sim \sqrt{2.8} \times \sigma_{\mathrm{RPC}} \sim 80\text{–}100 \text{ ps}.$$

The #p.e. generated by MIP depends on the material type and thickness. The PICOSEC collaboration reported about

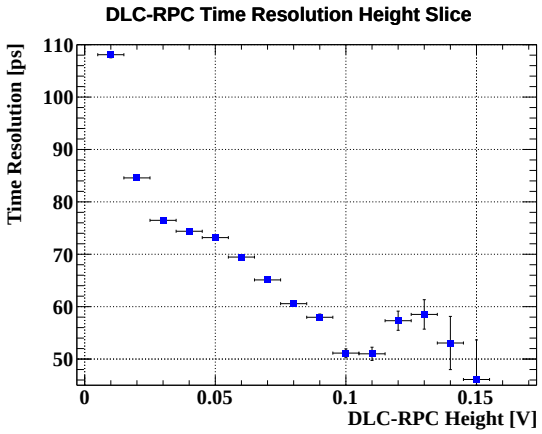

Figure 2. Time resolution of DLC-RPC sliced by signal height.

10 photoelectrons obtained from a 3 mm thick MgF_2 radiator and an 18 nm thick CsI photocathode with 3 nm thick Cr in between [7]. Considering 10 photoelectrons for the Cherenkov detector, the time resolution would be approximately 20–30 ps.

4 Measurement Setup

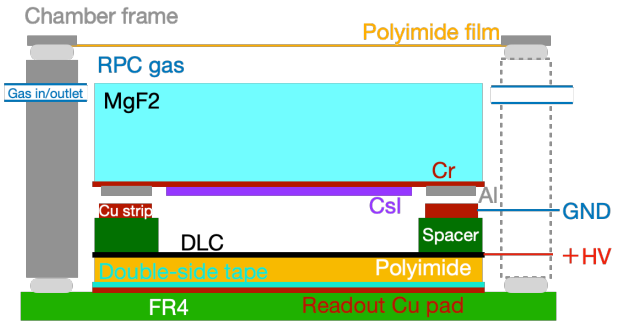

Figure 3. Schematic view of the prototype detector (not to scale)

A prototype detector has been constructed to demonstrate the detector concept. The primary goal was to observe the signal from Cherenkov light.

Figure 3 shows the schematic cross-section of the prototype detector, and its geometries are summarized in Table 1. A 4×4 cm^2 and 2.4 mm thick MgF_2 crystal was used as the radiator. A 3 nm thick Cr layer was vapor-deposited on the bottom face of the radiator, and an 18 nm thick CsI layer was deposited on the central 3×3 cm^2 area of the Cr layer as the semitransparent photocathode. MgF_2 has good transparency down to wavelengths of approximately 110 nm, and CsI is sensitive in the region below 200 nm. The choice of materials aims to maximize #p.e. An aluminum contact layer was deposited on the edge region of the Cr surface to ensure good contact with the ground-connected Cu strip. This Cu strip, whose thickness was 50 μm, was placed on top of the spacer, defining the gap thickness of the RPC. Due to the difficulty of making a thin spacer, the initial operation was conducted with a 350 μm gap thickness. The detector volume was enclosed in a chamber and a gas mixture same as DLC-RPC measurement shown in

Sec. 3. The top chamber window was made of polyimide film, and the bottom of the gas chamber was an FR-4 based PCB that reads out the signal induced on the Cu pad.

Table 1. Configuration of the prototype detector

	Material	Size
Radiator	MgF_2	2.4 mm-t
Photocathode	CsI	18 nm-t
Conductive layer	Cr	3 nm-t
Contact layer	Al	100 nm-t
Anode resistive layer	DLC	~ 100 nm-t
Active area	-	2×1 cm^2

The signal data were acquired using a waveform digitizer, WaveDREAM Board [8], with a factor 50 amplification and a 5 GHz sampling frequency. The initial operation was conducted by irradiating the detector with a ^{90}Sr β-ray source placed outside the polyimide film chamber window. A reference counter made of a SiPM-coupled scintillator was placed beneath the PCB of the prototype detector to trigger the events. In addition to β-ray data, cosmic-ray data were collected by placing another counter on top of the chamber window and triggering the events by the coincidence of two counters.

5 Result

5.1 Charge spectrum

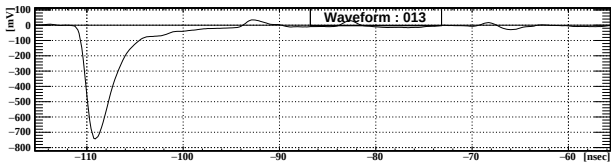

Figure 4. Typical waveform of the prototype detector irradiated with β-rays. From the signal size, it is most likely a 3 photoelectron event.

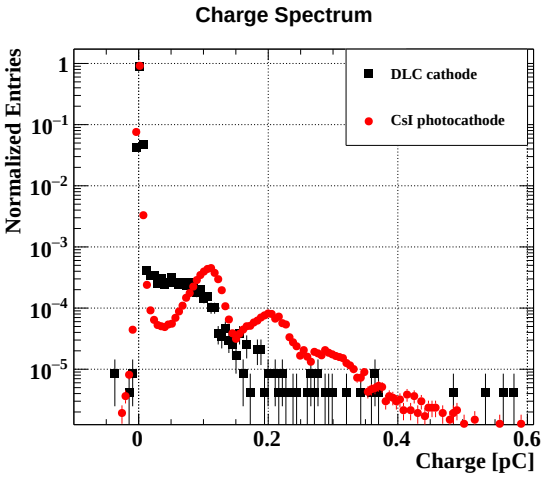

Figure 5. Charge spectrum of the 350 μm gap thickness prototype detector irradiated with β-rays. (Black) DLC cathode, (Red) CsI photocathode. The polarity of the signal is inverted in this plot. The entries are normalized by the number of triggered events.

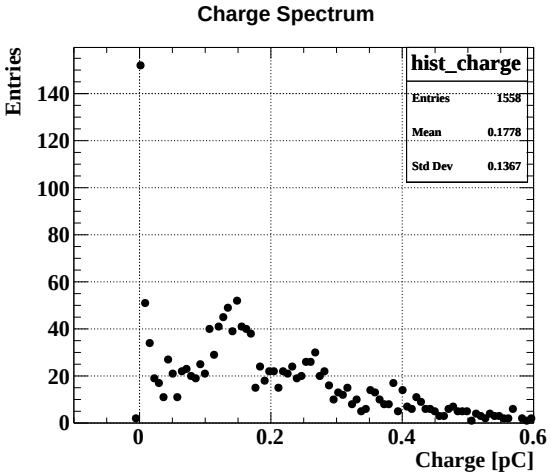

Figure 6. Cosmic-ray charge spectrum of the 350 μm gap thickness prototype detector.

The initial operation test of the prototype detector was conducted with a 350 μm gap thickness configuration ("CsI photocathode"). Figure 4 shows a sample waveform of the prototype detector. A similar configuration, except with the photocathode of the radiator replaced by DLC-sputtered polyimide foil as the cathode electrode ("DLC cathode"), was also tested. Essentially, "DLC cathode" configuration works as DLC-RPC. This was to determine whether the signals were originated from Cherenkov radiation or merely the ionization at the RPC gap.

Figure 5 compares the charge spectra of the two configurations for the ^{90}Sr β-rays. It is clear that the efficiency is significantly better for the "CsI photocathode" configuration, indicating the presence of Cherenkov signals. Additionally, there are multiple peak structures in the "CsI photocathode" charge spectrum that are absent in the other configuration. These peaks are considered to represent events with different numbers of photoelectrons. It was not able to obtain the efficiency of the prototype by this measurement because there were events triggered without β-ray passing the active region of the prototype.

The prototype detector was also tested with cosmic-rays. Figure 6 shows the charge spectrum for the cosmic rays. Due to the small acceptance and low flux, the statistics are limited. However, the multiple peak structures are still visible. The fraction of the signal charge over 0.05 pC was 79%. The average #p.e. is estimated to be 1.4 assuming a Poisson distribution.This is significantly smaller than the expectation of 10 p.e. as discussed in Sec. 3. The cause of the low #p.e. is under investigation.

5.2 Time resolution

After confirming stable operation, the time resolution was measured with a narrower 200 μm gap thickness configuration. Figure 7 shows the time resolution as a function of #p.e. for the prototype detector with 200 μm gap. The behavior of the plot fits well with two scenarios: a stochastic

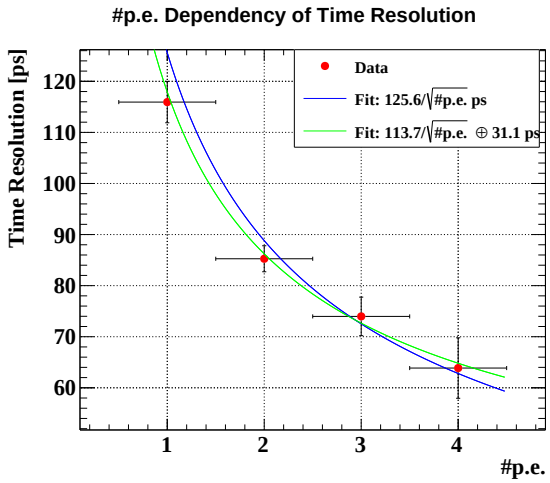

Figure 7. The time resolution as a function of #p.e. for the prototype detector with 200 μm gap measured with cosmic rays. The data points are fitted by two functions: 125.6/ $\sqrt{\#\text{p.e.}}$ (blue) and 113.7/ $\sqrt{\#\text{p.e.}}$ + 31.1 (green).

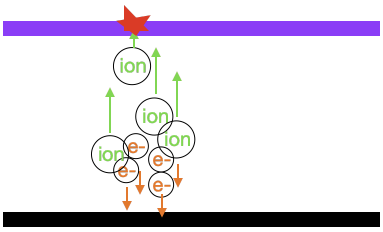

Figure 8. Schematic view of ion-backflow: Ions generated during the amplification drift to the surface of photocathode. The quantum efficiency of the photocathode can be deteriorated.

term by #p.e., with and without a constant term. If we extrapolate to #p.e. = 10, the time resolution will be 40 – 50 ps.

5.3 Operation issues

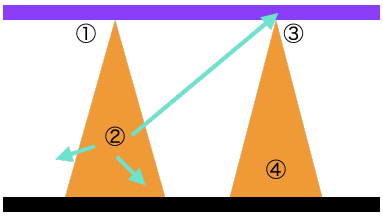

Figure 9. Schematic view of photon-feedback: (1) Cherenkov photons are converted to photoelectrons, which are then multiplied at the RPC gap. (2) During the amplification, excited molecules emit photons to de-excite. (3) Some of the photons generated in phase (2) hit the photocathode. (4) This causes a delayed avalanche and distorts the signal shape.

Even though the prototype detector successfully operated as a Cherenkov detector, its timing performance was worse than expected. This is primarily due to two issues. One is the small #p.e., and the other is the poorer single photoelectron time resolution.

The first issue is likely due to the deterioration of the quantum efficiency of the photocathode caused by ion-backflow (Figure 8). A robust photocathode such as DLC is being considered to replace CsI.

For the second issue, multiple factors could be contributing: distortion of the waveform by photon feedback (Figure 9), non-uniformity of the electric field in the gap due to unevenness of the anode electrode, and contamination of the signal from direct ionization in RPC gap. The main cause is still under investigation.

6 Conclusions

In this paper, we present a Cherenkov detector concept for the active layer of next-generation calorimetry that combines dual-readout and high granularity with picosecond-timing. We observed signals from the first prototype of the Cherenkov detector although important issues such as the ion-backflow and the photon-feedback need to be solved.

This research is supported by U.S.–Japan Science Cooperation Program in High Energy Physics. We thank S. Ban, A. Ochi, A. Oya, H. Suzuki, M. Takahashi, and K. Yamamoto for useful discussions, and also HAMAMATSU Photonics K.K. for the production of the photocathode.

References

[1] S. Lee, M. Livan and R. Wigmans, "Dual-readout calorimetry", Rev. Mod. Phys. **90**, 025002 (2018) https://doi.org/10.1103/RevModPhys.90.025002

[2] M.A. Thomson, "Particle flow calorimetry and the PandoraPFA algorithm", NIMA **611**, 25-40 (2009) https://doi.org/10.1016/j.nima.2009.09.009

[3] T. Kamiyama, et al., "Development of High-granularity Dual-readout Calorimetry with psec Timing", *20th International Conference on Calorimetery in Particle Physics* (Tsukuba, Japan, 2024)

[4] P. Fonte, et al., "High-resolution RPCs for large TOF systems", NIMA **449**, (2000) 295 https://doi.org/10.1016/S0168-9002(99)01299-1

[5] K. Ieki, W. Li, A. Ochi, et al., "Prototype study of 0.1%X_0 and MHz/cm^2 tolerant Resistive Plate Chamber with Diamond-Like Carbon electrodes" NIMA **1064**, (2024) https://doi.org/10.1016/j.nima.2024.169375.

[6] W. Riegler, C. Lippmann, and R. Veenhof, "Detector physics and simulation of resistive plate chambers," NIMA **500**, No. 1, 144-162 (2003) https://doi.org/10.1016/S0168-9002(03)00337-1

[7] J. Bortfeldt, F. Brunbauer, C. David, et al., "PICOSEC: Charged particle timing at sub-25 picosecond precision with a Micromegas based detector" NIMA **903**, 317-325 (2018) https://doi.org/10.1016/j.nima.2018.04.033

[8] L. Galli, A. Baldini, F. Cei, et al., "WaveDAQ: An highly integrated trigger and data acquisition system," NIMA **936**, 399-400 (2019) https://doi.org/10.1016/j.nima.2018.07.067